Available online at www.sciencedirect.com
ScienceDirect
International Journal of Heat and Mass Transfer 50 (2007) 1500–1515
International Journal of HEAT and MASS TRANSFER
www.elsevier.com/locate/ijhmt

Modeling of turbulent heat transfer and thermal dispersion for flows in flat plate heat exchangers

F. Pinson [a], O. Gregoire [a,*], M. Quintard [b], M. Prat [b], O. Simonin [b]

[a] CEA Saclay, DEN/DM2S/SFME, 91191 Gif sur Yvette Cedex, France
[b] IMFT, UMR CNRS/INP/UPS, Allée du Professeur Camille Soula, 31400 Toulouse, France

Received 15 February 2006; received in revised form 20 July 2006
Available online 7 November 2006

Abstract

In this paper, heat transfer and dispersion for both laminar and turbulent regimes in heat exchangers and nuclear cores are considered. Such hydraulic systems might be seen as spatially periodic porous media. The existence of a turbulent flow within a porous medium structure suggests the use of a spatial average operator, combined to a statistical average operator. Previous works [M.H.J. Pedras, M.J.S. De Lemos, Macroscopic turbulence modeling for incompressible flow through undeformable porous media, Int. J. Heat Mass Transfer 44 (2001) 1081–1093; F. Kuwahara, A. Nakayama, H. Koyama, A numerical study of thermal dispersion in porous medium, J. Heat Transfer 118 (1996) 756–761] have applied a double average procedure to the thermal balance equation, which led to a macroscopic turbulent transport and a subsequent macro-scale equation featuring dynamic dispersion. Considering the heat flux at the solid surfaces as a boundary condition for the fluid energy balance, the model proposed in this paper allows one to take into account this dispersion as the sum of two contributions. The first one is the classical dispersion due to velocity heterogeneities [G. Taylor, Dispersion of solute matter in solvent flowing slowly through a tube, Proc. Roy. Soc. Lond. A 219 (1953) 186–203] and the second one is due to wall heat transfer. Applying Whitaker up-scaling method [S. Whitaker, Theory and applications of transport in porous media: the method of volume averaging, Kluwer Academic Publishers, 1999], a "closure problem" is then derived for a representative elementary volume, using the so-called Boussinesq approximation to account for small scale turbulence. The model is used to compute macro-scale heat transfer properties for turbulent flows inside a flat plate heat exchanger. It is shown that, for such flows, both dispersive fluxes strongly predominate over the macroscopic turbulent heat flux.

Keywords: Thermal dispersion; Turbulence; Spatial average; Double averaging; Porous media; Heat exchangers

1. Introduction

The overall objective of this paper is the macro-scale description of heat transfer and dispersion in heat exchangers and nuclear reactors [5]. Indeed, the geometrical complexity of such systems does not allow to calculate the details of the velocity and temperature profiles within each subchannel [6]. A practical way to avoid this difficulty is to consider a large scale (hereafter denoted "macroscopic") description of the convection–diffusion phenomena rather than giving focus on the fine ("microscopic") description of the flow [3]. Such a macroscopic description may be derived from the microscopic flow equations, at the pore-scale, through some up-scaling methods. This generally results into modified equations for mean flow variables, with additional contributions like dispersion, tortuosity and other transfer terms that account for small scale phenomena. We will refer to such methods as porous media type of analysis. Originally, these methods have been developed to model creeping flows within "micro-porous media" characterized by very small pore sizes [7]. Nevertheless, dispersion is also a subject of great interest for "macro-porous media" like heat exchangers, with the additional difficulty

* Corresponding author. Tel.: +33 1 69 08 22 85; fax: +33 1 69 08 85 68.
E-mail address: olivier.gregoire@cea.fr (O. Gregoire).

0017-9310/$ - see front matter © 2006 Elsevier Ltd. All rights reserved.
doi:10.1016/j.ijheatmasstransfer.2006.08.033

Nomenclature

A_f	interface between solid and fluid phases (m^2)
$\mathscr{C}_A, \mathscr{C}_P, \mathscr{C}_v$	constants
C_μ, C_{ϵ_1}, C_{ϵ_2}	constants of the k–ϵ model
D_H	mean hydraulic diameter of the pores (m)
$\mathscr{D}^P$	thermal passive dispersion tensor ($m^2\ s^{-1}$)
$\mathscr{D}^A$	thermal active dispersion vector (m)
f_p	friction coefficient
f_μ, f_2	damping functions in the low-Reynolds k–ϵ model
h	local heat transfer coefficient ($W\ m^{-2}\ K^{-1}$)
l	microscopic characteristic length scale (m)
L	macroscopic characteristic length scale (m)
n_i	ith component of the interface normal vector, pointing towards the solid phase
Pe	$\langle \bar{u} \rangle_f D_H/\alpha_f$, Péclet number
Pr	v/α_f, Prandtl number
Pr_t	v_t/α_t, turbulent Prandtl number
P_w	wetted perimeter (m)
r_0	representative elementary volume length scale (m)
$(\rho c_p)_f$	specific heat of the fluid phase ($J\ m^{-3}\ K^{-1}$)
Re	$D_H \langle \bar{u} \rangle_f / v$, pore Reynolds number
Re_t	v_t/v, turbulence Reynolds number
S_w	flow area (m^2)
T_f	fluid temperature (K)
T_w	wall temperature (K)
u_f	$\sqrt{v \cdot \frac{\partial u}{\partial n}\|_{wall}}$, friction velocity ($m\ s^{-1}$)
u_i	ith component of the fluid velocity ($m\ s^{-1}$)
$\langle \bar{u} \rangle_f$	bulk flow velocity ($m\ s^{-1}$)
u^+	$\bar{u}/u_f$, normalized velocity
ΔV	representative elementary volume (REV) (m^3)
ΔV_f	fluid volume included in the REV (m^3)
y^+	normalized distance to the wall

Greek symbols

α_f	thermal diffusivity of the fluid ($m^2\ s^{-1}$)
α_t	turbulent thermal diffusivity ($m^2\ s^{-1}$)
α_{t_M}	macroscopic turbulent thermal diffusivity ($m^2\ s^{-1}$)
χ_f	fluid characteristic function
δ_t	conductive boundary layer thickness (m)
δ_w	Dirac delta function associated to the interface (m^{-1})
δ_v	viscous boundary layer thickness (m)
η_i	ith component of the dispersion function related to the mean temperature gradient (m)
ζ	dispersion function related to the wall heat flux (s)
ϕ	porosity of the medium
v	kinematic viscosity of the fluid ($m^2\ s^{-1}$)
v_t	turbulent kinematic viscosity ($m^2\ s^{-1}$)
Φ	heat flux at the fluid solid interface ($W\ m^{-2}$)
ρ	density of the fluid ($kg\ m^{-3}$)
ω_i	ith component of the interface velocity ($m\ s^{-1}$)
σ_k	turbulent Schmidt number associated to k
σ_ϵ	turbulent Schmidt number associated to ϵ
τ	characteristic evolution time of $\delta\overline{T_f}$ (s)
τ_d	D_H^2/α_f, characteristic thermal diffusion time (s)

Additional notations

$\langle \cdot \rangle$	volume average
$\langle \cdot \rangle_f$	fluid volume average
$\delta\cdot$	deviation from the fluid volume average
$\bar{\cdot}$	statistical average
$\cdot'$	fluctuation from the statistical average
$\cdot^*$	dimensionless quantity

that turbulent flows may occur within the pores, as pointed out by Taylor [8].

One of the leading ideas of up-scaling methods is to derive the macro-scale properties for a representative elementary volume (REV). Approximate solutions (closure problems) of the coupled micro-scale and macro-scale (averaged) equations were found for the dispersion problem through various approaches: volume averaging [4,9], homogenization [10,11] or moments methods [12]. Within the laminar regime, and for simple geometries, it is possible to analytically solve the closure problems to calculate the dispersion tensors and other effective parameters. For more complex geometries, even for laminar flows, numerical models may be required. These results cannot be used directly for modeling macroscopically heat exchangers since flows in such systems are generally turbulent. The specificity of the turbulent regime is that, even for very simple geometries like channel or pipe flows, one cannot analytically solve the Navier Stokes equations.

Within the framework of the double decomposition formalism [1,2], we present an analysis of thermal dispersion and heat transfer for turbulent flows in heat exchangers. Hence, the hydraulic systems which are considered in this work are stratified porous media. Following the ideas implemented in reactor subchannel analysis codes (FLICA4 [5], COBRA-IIIC, SABRE, ... [6]), we choose to combine the resolution for the spatially averaged fluid temperature with a fine scale resolution for the solid temperature. In the following, this approach will be denoted "mixed model". Thus, the solid phase is seen from the fluid phase as a heat source/sink term, while the fluid phase provides boundary conditions for the fine scale temperature calculation in the solid. In this paper, we focus on the fluid temperature modeling. Therefore, we will consider that thermal interactions with solids reduce to an external forcing for the fluid temperature. Let us emphasize that the mixed model is relevant when the fluid and solid exhibit really different characteristic time scales. This is the case

in nuclear reactors under normal operating condition where heat source is provided by nuclear reactions.

Sections 2 and 3 are devoted to the derivation of the balance equation for the mean fluid density and temperature respectively. The properties of both statistical and spatial averages used in these sections are recalled in Appendix A. After the simplification of the temperature deviation balance equation, a closure problem for temperature dispersion is presented in Section 5. The modelization of temperature deviation is addressed in the same section. Then, the proposed set of equations is applied to the thermal dispersion inside a flat plate heat exchanger, for laminar flows in Section 7 and for turbulent flows in Section 8. A comparison with Taylor analysis [8] is presented in the same section.

2. Derivation of the averaged continuity equation

We consider an incompressible, single phase flow in a saturated, rigid porous medium. Fluid properties are assumed constant and a no-slip velocity condition at the wall is used. The spatial variation of the porosity is supposed to be in accordance with the variation length-scale constraints discussed in A.2. The turbulence study suggests the use of a statistical or time average, denoted "$\bar{\cdot}$", while the porous structure calls for the use of fluid volume average, denoted "$\langle\cdot\rangle_f$" Fig. 1. Pedras and De Lemos [1] performed an extensive study of the double-averaging procedure. In this context, let ξ be any physical quantity, one can write

$$\xi = \langle\bar{\xi}\rangle_f + \langle\xi'\rangle_f + \delta\bar{\xi} + \delta\xi' \tag{1}$$

with the definitions:

$$\xi = \bar{\xi} + \xi' \quad \text{and} \quad \xi = \langle\xi\rangle_f + \delta\xi. \tag{2}$$

In [1], it is demonstrated that both operators commute. This allows the use of the time–space or space–time averaging sequences without information loss. Nevertheless, Travkin [13] claimed that, even if this property is true in a strict mathematical point of view, it could have practical consequences on the development of the physical model. Applying first spatial filtering, with a characteristic scale larger than the pore size, will require that the small eddies must be modeled in the averaged equations [14] while the dynamic of big eddies is expected to be conserved in the large-scale behavior of these averaged equations. Therefore, the application of the statistical filter on the averaged equations would only permit a treatment of the large scale turbulence. If small-scale eddies are important, i.e. turbulence at a scale lower than the pore size, it is more attractive to first apply the statistical average. Under these circumstances, this first averaging procedure leads to a readily interpretable step thanks to the amount of knowledge achieved in turbulence modelization. Classical turbulent models can be used to describe flows within channels, and spatial averaging may be used subsequently. Given the fact that, in the cases that motivated our study, turbulence can be considered as developed within the pores, we choose to apply statistical averaging in a first step and the volume averaging in a second step.

The microscopic continuity equation for an incompressible, non-reactive flow is given by

$$\frac{\partial u_i}{\partial x_i} = 0 \tag{3}$$

with a no-slip boundary condition at the walls

$$u_i = 0 \quad \text{on } A_f. \tag{4}$$

Applying the statistical average, we obtain

$$\frac{\partial \overline{u_i}}{\partial x_i} = 0. \tag{5}$$

We now apply the volume average and use the theorem of local averaging (see Appendix A, Eq. (A.9)) to obtain

$$\frac{\partial \phi\langle\overline{u_i}\rangle_f}{\partial x_i} + \langle\overline{u_i} n_i \delta_w\rangle = 0. \tag{6}$$

All notations and theorems used in this paper are summarized in Appendix A. The no-slip boundary condition (4) requires the second term of the left hand side to be zero. Hence, the macroscopic continuity equation reads

$$\frac{\partial}{\partial x_i}\phi\langle\overline{u_i}\rangle_f = 0. \tag{7}$$

One can also note that, splitting the velocity into its spatial average value and its deviation in relation (5), we obtain the following relation

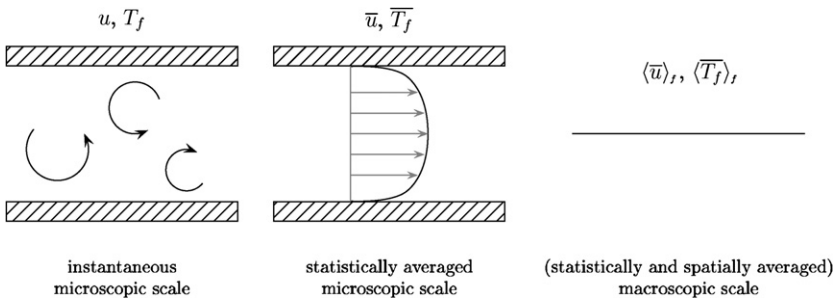

Fig. 1. Description of three scales in the single channel case. The statistical average allows to get a structured view of the flow whereas the spatial average allows to get a one-dimensional description of the single channel.

$$\frac{\partial\langle\overline{u_i}\rangle_f}{\partial x_i} = -\frac{\partial\delta\overline{u_i}}{\partial x_i} = -\frac{\langle\overline{u_i}\rangle_f}{\phi}\frac{\partial\phi}{\partial x_i}. \tag{8}$$

3. Averaged fluid temperature equation

For constant fluid properties (density, viscosity and heat capacity), the instantaneous microscopic heat balance equation reads

$$\frac{\partial T_f}{\partial t} + \frac{\partial u_i T_f}{\partial x_i} = \frac{\partial}{\partial x_i}\left(\alpha_f \frac{\partial T_f}{\partial x_i}\right) \tag{9}$$

and the corresponding boundary condition on the wall A_f

$$\alpha_f \frac{\partial T_f}{\partial x_i} n_i = \frac{\Phi}{(\rho c_p)_f}. \tag{10}$$

The first averaging procedure, i.e., the statistical average, leads to the classical equation involving a turbulent heat flux

$$\frac{\partial\overline{T_f}}{\partial t} + \frac{\partial\overline{u_i}\,\overline{T_f}}{\partial x_i} = -\frac{\partial}{\partial x_i}\underbrace{\overline{u_i' T_f'}}_{\substack{\text{Turbulent}\\ \text{heat flux}}} + \frac{\partial}{\partial x_i}\left(\alpha_f \frac{\partial\overline{T_f}}{\partial x_i}\right). \tag{11}$$

In the Reynolds averaged Navier Stokes (RANS) context, the turbulent heat flux is usually modeled according to a generalized Fick's law

$$\overline{u_i' T_f'} = -\alpha_t \frac{\partial\overline{T_f}}{\partial x_i}. \tag{12}$$

where α_t is the turbulent thermal diffusivity. This model is called the first gradient approximation. Now, the modeled equation for the statistically averaged temperature reads

$$\frac{\partial\overline{T_f}}{\partial t} + \frac{\partial\overline{u_i}\,\overline{T_f}}{\partial x_i} = \frac{\partial}{\partial x_i}\left(\alpha_f \frac{\partial\overline{T_f}}{\partial x_i}\right) + \frac{\partial}{\partial x_i}\left(\alpha_t \frac{\partial\overline{T_f}}{\partial x_i}\right), \tag{13}$$

$$\alpha_f \frac{\partial\overline{T_f}}{\partial x_i} n_i = \frac{\overline{\Phi}}{(\rho c_p)_f} \quad \text{on } A_f. \tag{14}$$

Because of the spatial dependance of α_t, this problem is reminiscent of previous work on spatially variable dispersion tensors [15].

Applying the volume average to (13), we obtain the following equation for the mean flow temperature:

$$\begin{aligned}\phi\frac{\partial\langle\overline{T_f}\rangle_f}{\partial t} &+ \frac{\partial\phi\langle\overline{u_i}\rangle_f\langle\overline{T_f}\rangle_f}{\partial x_i}\\ &= \frac{\partial}{\partial x_i}\left(\phi\alpha_f\frac{\partial\langle\overline{T_f}\rangle_f}{\partial x_i}\right) + \frac{\partial}{\partial x_i}\left(\phi\left\langle\alpha_t\frac{\partial\overline{T_f}}{\partial x_i}\right\rangle_f\right)\\ &+ \underbrace{\left\langle\alpha_f\frac{\partial\overline{T_f}}{\partial x_i}n_i\delta_w\right\rangle}_{\text{Wall heat transfer}} \underbrace{-\frac{\partial}{\partial x_i}\phi\langle\delta\overline{u_i}\delta\overline{T_f}\rangle_f}_{\text{Thermal dispersion}} + \underbrace{\frac{\partial}{\partial x_i}\phi\langle\alpha_f\delta\overline{T_f}n_i\delta_w\rangle_f}_{\text{Tortuosity}}.\end{aligned} \tag{15}$$

The dispersion and the tortuosity terms are typical of the porous medium approach. For high Péclet number flows, the macroscopic convective term predominates over the tortuosity term [2]. In addition, the spatially averaged thermal turbulent flux can be modeled through the definition of a macroscopic turbulent thermal conductivity α_{t_M} [1,14]:

$$\left\langle\alpha_t\frac{\partial\overline{T_f}}{\partial x_i}\right\rangle_f \equiv \alpha_{t_M}\frac{\partial\langle\overline{T_f}\rangle_f}{\partial x_i}. \tag{16}$$

Let us note that one could avoid this additive closure relation by decomposing the temperature in its averaged and deviation parts and thus directly close the deviation part. However, this approach results The thermal volume source term ($W\,m^{-3}$), induced by thermal conduction at walls, reads

$$\left\langle\alpha_f\frac{\partial\overline{T_f}}{\partial x_i}n_i\delta_w\right\rangle = \frac{\langle\overline{\Phi}\delta_w\rangle}{(\rho c_p)_f} = \phi\frac{\langle\overline{\Phi}\delta_w\rangle_f}{(\rho c_p)_f}. \tag{17}$$

Finally, the evolution of the statistically and spatially averaged temperature is given by

$$\begin{aligned}\phi\frac{\partial\langle\overline{T_f}\rangle_f}{\partial t} &+ \frac{\partial\phi\langle\overline{u_i}\rangle_f\langle\overline{T_f}\rangle_f}{\partial x_i}\\ &= \frac{\partial}{\partial x_i}\left[\phi(\alpha_f+\alpha_{t_M})\frac{\partial\langle\overline{T_f}\rangle_f}{\partial x_i}\right] + \phi\frac{\langle\overline{\Phi}\delta_w\rangle_f}{(\rho c_p)_f}\\ &- \frac{\partial}{\partial x_i}\phi\langle\delta\overline{u_i}\delta\overline{T_f}\rangle_f + \frac{\partial}{\partial x_i}\phi\langle\alpha_f\delta\overline{T_f}n_i\delta_w\rangle_f.\end{aligned} \tag{18}$$

In Eq. (18), three terms remain unknown and need to be modeled: the macroscopic turbulent heat flux, the thermal dispersion and the tortuosity. We underline that dispersion is induced by the coupling between velocity and temperature deviations.

4. Temperature deviation equation

In order to model the tortuosity and the thermal dispersion terms in the mean temperature equation, we follow Whitaker's methodology [16] and extend the so-called "closure problem" to the case of microscopic turbulent flows. Within this approach, one must first derive the evolution equation for the spatial temperature deviation. Two major assumptions will contribute to the model design:

H1. The assumption of scale separation, often written as

$$L \gg l.$$

Let us consider any quantity ξ that satisfies the property

$$\delta\xi = O(\langle\xi\rangle_f),$$

then the hypothesis H1 among others implies that the space derivative of the deviation rules over the spatial derivative of the macroscopic quantity, namely

$$\underbrace{\frac{\partial\delta\xi}{\partial x_i}}_{o\left(\frac{\delta\xi}{l}\right)} \gg \underbrace{\frac{\partial\langle\xi\rangle_f}{\partial x_i}}_{o\left(\frac{\langle\xi\rangle_f}{L}\right)}. \tag{19}$$

H2. The evolution of the temperature deviation is supposed to be quasi-steady with respect to the forcing

term, which is the evolution of the averaged temperature. This condition could be written

$$\frac{l^2}{\alpha_f} \ll \frac{L^2}{\alpha_f} \tag{20}$$

and we see that it is satisfied from assumption H1.

To obtain the temperature deviation equation, we substract the macroscopic heat Eq. (18) from the statistically averaged microscopic one (Eq. (13)),

$$\begin{aligned}&\frac{\partial \delta\overline{T_f}}{\partial t} + \frac{\partial}{\partial x_i}(\overline{u_i}\delta\overline{T_f}) \\ &= \frac{\partial}{\partial x_i}\left(\alpha_f \frac{\partial \delta\overline{T_f}}{\partial x_i}\right) + \frac{\partial}{\partial x_i}\left(\alpha_t \frac{\partial \overline{T_f}}{\partial x_i} - \alpha_{t_M}\frac{\partial \langle\overline{T_f}\rangle_f}{\partial x_i}\right) + \frac{\partial}{\partial x_i}\langle\delta\overline{u_i}\delta\overline{T_f}\rangle_f \\ &\quad - \frac{\partial}{\partial x_i}\left(\delta\overline{u_i}\langle\overline{T_f}\rangle_f\right) - \frac{\partial}{\partial x_i}\langle\alpha_f \delta\overline{T_f} n_i \delta_w\rangle_f - \frac{\langle\overline{\Phi}\delta_w\rangle_f}{(\rho c_p)_f}\end{aligned} \tag{21}$$

with the following boundary condition on A_f

$$\alpha_f\left[\frac{\partial\langle\overline{T_f}\rangle_f}{\partial x_i} + \frac{\partial\delta\overline{T_f}}{\partial x_i}\right]n_i = \frac{\overline{\Phi}}{(\rho c_p)_f}. \tag{22}$$

The orders of magnitude for each contribution in Eq. (21) have been estimated and are summarized in Table 1. The order of magnitude of the velocity deviation with respect to the mean velocity is deduced from the no-slip boundary condition. Since we have at walls

$$\overline{u_i} = 0 \quad \text{on } A_f \Longleftrightarrow \langle\overline{u_i}\rangle_f = \delta\overline{u_i} \quad \text{on } A_f, \tag{23}$$

we get [4]:

$$\langle\bar{u}\rangle_f = O(\delta\bar{u}) \quad \text{in } \Delta V_f. \tag{24}$$

In the same way, one could write for the turbulent thermal flux:

$$\begin{aligned}&\alpha_t\frac{\partial\overline{T_f}}{\partial x_i} = 0 \quad \text{on } A_f \Rightarrow \alpha_{t_M}\frac{\partial\langle\overline{T_f}\rangle_f}{\partial x_i} = \left\langle\alpha_t\frac{\partial\overline{T_f}}{\partial x_i}\right\rangle_f \\ &= O\left(\delta\left(\alpha_t\frac{\partial\overline{T_f}}{\partial x_i}\right)\right) \quad \text{in } \Delta V_f.\end{aligned} \tag{25}$$

Table 1
Magnitude order of the terms in relation (21)

	Terms of Eq. (21)	Order of magnitude
I	$(\rho c_p)_f\frac{\partial\delta\overline{T_f}}{\partial t}$	$\frac{(\rho c_p)_f\delta\overline{T_f}}{\tau}$
II	$(\rho c_p)_f\frac{\partial}{\partial x_i}(\overline{u_i}\delta\overline{T_f})$	$(\rho c_p)_f(\langle\bar{u}\rangle_f + \delta\bar{u})\frac{\delta\overline{T_f}}{l}$
III	$\frac{\partial}{\partial x_i}\left(\alpha_f\frac{\partial\delta\overline{T_f}}{\partial x_i}\right)$	$\alpha_f\frac{\delta\overline{T_f}}{l^2}$
IV	$(\rho c_p)_f\frac{\partial}{\partial x_i}\langle\overline{u_i'T_f'}\rangle_f$	$(\rho c_p)_f\frac{\langle\overline{u'T_f'}\rangle_f}{L}$
V	$(\rho c_p)_f\frac{\partial}{\partial x_i}(\overline{u_i'T_f'})$	$(\rho c_p)_f\frac{\overline{u'T_f'}}{l}$
VI	$(\rho c_p)_f\frac{\partial}{\partial x_i}\langle\delta\overline{u_i}\delta\overline{T_f}\rangle_f$	$(\rho c_p)_f\frac{\delta\bar{u}\delta\overline{T_f}}{L}$
VII	$(\rho c_p)_f\frac{\partial}{\partial x_i}(\delta\overline{u_i}\langle\overline{T_f}\rangle_f)$	$(\rho c_p)_f\frac{\delta\bar{u}\langle\overline{T_f}\rangle_f}{L}$
VIII	$\frac{\partial}{\partial x_i}\langle\alpha_f\delta\overline{T_f}n_i\delta_w\rangle_f$	$\alpha_f\frac{\delta\overline{T_f}}{L^2}$ [31]

We recall here that these latter estimations (Eqs. (24) and (25)) are necessary to apply the H1 hypothesis. Then, according to Table 1, it is possible to neglect terms IV, VI and VIII by comparing them with terms V, II and III respectively. Concerning the temperature, we see that the macroscopic gradient has a leading role in relation (21). This remark is reminiscent of what has been found in the study of passive scalar dispersion [16]. The macroscopic temperature gradient must be preserved in the boundary condition (22). Furthermore, hypothesis H2 leads to remove term I from Eq. (21).

The turbulent heat flux in Eq. (21) is decomposed according to its macroscopic contribution and its deviation. Its macroscopic part can then be developed and simplified thanks to the H1 hypothesis:

$$\begin{aligned}\frac{\partial}{\partial x_i}\left(\alpha_t\frac{\partial\langle\overline{T_f}\rangle_f}{\partial x_i}\right) &= \underbrace{\alpha_t\frac{\partial^2\langle\overline{T_f}\rangle_f}{\partial x_i\partial x_i}}_{o\left(\frac{\alpha_t\langle\overline{T_f}\rangle_f}{L^2}\right)} + \underbrace{\frac{\partial\alpha_t}{\partial x_i}\frac{\partial\langle\overline{T_f}\rangle_f}{\partial x_i}}_{o\left(\frac{\alpha_t\langle\overline{T_f}\rangle_f}{Ll}\right)} \\ &\simeq \frac{\partial\alpha_t}{\partial x_i}\frac{\partial\langle\overline{T_f}\rangle_f}{\partial x_i}.\end{aligned} \tag{26}$$

Thanks to the zero velocity divergence for incompressible flow, the simplified form of Eq. (21) for microscopic turbulent flows finally reads

$$\begin{aligned}&\overline{u_i}\frac{\partial\delta\overline{T_f}}{\partial x_i} - \frac{\partial}{\partial x_i}\left((\alpha_f + \alpha_t)\frac{\partial\delta\overline{T_f}}{\partial x_i}\right) \\ &= \left(\frac{\partial\alpha_t}{\partial x_i} - \delta\overline{u_i}\right)\frac{\partial\langle\overline{T_f}\rangle_f}{\partial x_i} - \frac{\langle\overline{\Phi}\delta_w\rangle_f}{(\rho c_p)_f}\end{aligned} \tag{27}$$

with the following boundary condition on A_f

$$\alpha_f\frac{\partial\delta\overline{T_f}}{\partial x_i}n_i = \frac{\overline{\Phi}}{(\rho c_p)_f} - \alpha_f\frac{\partial\langle\overline{T_f}\rangle_f}{\partial x_i}n_i. \tag{28}$$

5. Dispersion closure problem in periodic unit cells

In Eq. (27), let us note that the left hand side linearly depends on the macroscopic temperature gradient $(\partial\langle\overline{T_f}\rangle_f/\partial x_i)$ and the mean thermal source term $(\langle\overline{\Phi}\delta_w\rangle_f/(\rho c_p)_f)$. These are the source terms of the temperature deviation balance equation. This analysis and the literature survey discussed in the introduction lead us to look for a closure relationship of the form:

$$\delta\overline{T_f} = \eta_i\frac{\partial\langle\overline{T_f}\rangle_f}{\partial x_i} + \zeta\frac{\langle\overline{\Phi}\delta_w\rangle_f}{(\rho c_p)_f} + \psi. \tag{29}$$

Carbonell and Whitaker [17] have shown that the function ψ, that can account for spatial disorder of the media at the microscopic scale, is zero for periodic porous media. The dispersion functions η_j (homogeneous to a length) and ζ (homogeneous to a time) are local quantities. A relation for the functions η_i and ζ can be deduced from the idempotence property of the averaging operator

$$\langle \delta\overline{T_f}\rangle_f = 0 \quad \Longleftrightarrow \quad \langle \eta_i\rangle_f \frac{\partial\langle\overline{T_f}\rangle_f}{\partial x_i} + \langle\zeta\rangle_f \frac{\langle\overline{\Phi}\delta_w\rangle_f}{(\rho c_p)_f} = 0. \tag{30}$$

The same simplification than the one presented in (26) again applies to determine the successive derivatives of the modeled temperature deviation:

$$\frac{\partial\delta\overline{T_f}}{\partial x_i} \simeq \frac{\partial\eta_j}{\partial x_i}\frac{\partial\langle\overline{T_f}\rangle_f}{\partial x_j} + \frac{\partial\zeta}{\partial x_i}\frac{\langle\overline{\Phi}\delta_w\rangle_f}{(\rho c_p)_f}, \tag{31}$$

$$\frac{\partial}{\partial x_i}\left[(\alpha_f+\alpha_t)\frac{\partial\delta\overline{T_f}}{\partial x_i}\right] \simeq \frac{\partial}{\partial x_i}\left[(\alpha_f+\alpha_t)\frac{\partial\eta_j}{\partial x_i}\right]\frac{\partial\langle\overline{T_f}\rangle_f}{\partial x_j} + \frac{\partial}{\partial x_i}\left[(\alpha_f+\alpha_t)\frac{\partial\zeta}{\partial x_i}\right]\frac{\langle\overline{\Phi}\delta_w\rangle_f}{(\rho c_p)_f}. \tag{32}$$

Substituting the modeled expression for the deviation in the boundary condition (22) leads to the following boundary conditions for the derivatives of the dispersion functions

$$\alpha_f\left(\frac{\partial\eta_j}{\partial x_i}+\delta_{ij}\right)\frac{\partial\langle\overline{T_f}\rangle_f}{\partial x_j}n_i + \alpha_f\frac{\partial\zeta}{\partial x_i}\frac{\langle\overline{\Phi}\delta_w\rangle_f}{(\rho c_p)_f} = \frac{\overline{\Phi}}{(\rho c_p)_f}. \tag{33}$$

The relation (33) is a general expression relating the wall heat flux to the macroscopic temperature gradient and the derivatives of the dispersion functions. In order to recover the passive dispersion closure problem when $\overline{\Phi}$ tends toward zero, the two closure problems for η and ζ should not be coupled. We assume that, at the boundary, the heat flux is only related to the ζ gradient, such that we have

$$\frac{\partial\eta_j}{\partial x_i}+\delta_{ij}=0 \quad \text{and} \quad \alpha_f\frac{\partial\zeta}{\partial x_i}\frac{\langle\overline{\Phi}\delta_w\rangle_f}{(\rho c_p)_f}n_i = \frac{\overline{\Phi}}{(\rho c_p)_f} \quad \text{on } A_f. \tag{34}$$

Now, we define the vector **p** which characterize the periodic property of the porous media. By substituting the modeled expression for the fluid temperature deviation (29) in Eq. (27) and by using the simplification of the modeled temperature deviation derivatives (Eqs. (31) and (32)), the closure problem for a periodic unit cell can be specified

$$\text{inside the REV:} \quad \overline{u_i}\frac{\partial\eta_j}{\partial x_i} - \frac{\partial}{\partial x_i}\left[(\alpha_f+\alpha_t)\frac{\partial\eta_j}{\partial x_i}\right] = \frac{\partial\alpha_t}{\partial x_j} - \delta\overline{u_j}, \tag{35}$$

$$\overline{u_i}\frac{\partial\zeta}{\partial x_i} - \frac{\partial}{\partial x_i}\left[(\alpha_f+\alpha_t)\frac{\partial\zeta}{\partial x_i}\right] = -1, \tag{36}$$

$$\text{on } A_f: \quad \frac{\partial\eta_j}{\partial x_i} = -\delta_{ij}, \tag{37}$$

$$\alpha_f\frac{\partial\zeta}{\partial x_i}n_i = \frac{\overline{\Phi}}{\langle\overline{\Phi}\delta_w\rangle_f}, \tag{38}$$

$$\text{periodicity:} \quad \eta_j(\mathbf{x}+p_i)=\eta_j(\mathbf{x}), \quad \zeta(\mathbf{x}+p_i)=\zeta(\mathbf{x}), \tag{39}$$

$$\text{additional relation:} \quad \langle\eta_j\rangle_f\frac{\partial\langle\overline{T_f}\rangle_f}{\partial x_j} + \langle\zeta\rangle_f\frac{\langle\overline{\Phi}\delta_w\rangle_f}{(\rho c_p)_f} = 0. \tag{40}$$

Each mapping variable, η_j and ζ, is described thanks to an advection diffusion equation with various source terms. The quantity η_j is governed by the spatial heterogeneities of the mean velocity field and the gradient of the turbulent thermal diffusion, whereas the budget of ζ is an up-scaled representation of the local heat transfer. The first mapping variable is analogous to the dispersion function encountered in passive scalar dispersion problems. If temperature was treated as a passive scalar or if we had considered thermal equilibrium between phases, only this contribution would remain. In this peculiar case, the additional relation (40) is in accordance with the passive scalar study. It gives $\langle\eta_j\rangle_f = 0$ [18]. The second term accounts for thermal non-equilibrium in the pore, due to the heat exchange at the solid surface. For flows satisfying the H1 assumption, the temperature deviation is mainly determined by the wall heat flux. Hence we infer that the second contribution is dominant.

Solving the system requires the knowledge of velocity and turbulent diffusivity profiles. For laminar flows in some simple geometries, the velocity profiles can be calculated analytically. Consequently, both dispersion functions can analytically be derived (see Section 7). For more complex geometries, even for the laminar regime, one can use a CFD code to obtain the detailed velocity profiles. The specificity of the turbulent regime is that one cannot analytically solve the Navier Stokes equations for most practical applications. We shall use models which more or less account for complex phenomena such as turbulence/wall interactions. As a consequence, we must remember that the results may slightly depend on the choice of the turbulence model.

At this stage, we have established the relation between the temperature deviation, the macroscopic temperature gradient and the volume averaged heat flux, by defining the two mapping variables (or dispersion functions) in Eq. (29). Substituting (29) in (18), we can clarify the modeled equation for the macroscopic temperature

$$\begin{aligned}\phi\frac{\partial\langle\overline{T_f}\rangle_f}{\partial t} + \frac{\partial\phi\langle\overline{u_i}\rangle_f\langle\overline{T_f}\rangle_f}{\partial x_i} &= \frac{\partial}{\partial x_i}\left(\phi(\alpha_f+\alpha_{t_M})\frac{\partial\langle\overline{T_f}\rangle_f}{\partial x_i}\right) + \phi\frac{\langle\overline{\Phi}\delta_w\rangle_f}{(\rho c_p)_f} \\ &\underbrace{-\frac{\partial}{\partial x_i}\left(\phi\langle\delta\overline{u_i}\eta_j\rangle_f\frac{\partial\langle\overline{T_f}\rangle_f}{\partial x_j}\right)}_{(a)} \underbrace{-\frac{\partial}{\partial x_i}\left(\phi\langle\delta\overline{u_i}\zeta\rangle_f\frac{\langle\overline{\Phi}\delta_w\rangle_f}{(\rho c_p)_f}\right)}_{(b)} \\ &+\underbrace{\frac{\partial}{\partial x_i}\left(\phi\langle\alpha_f\eta_j n_i\delta_w\rangle_f\frac{\partial\langle\overline{T_f}\rangle_f}{\partial x_j}\right)}_{(c)} + \underbrace{\frac{\partial}{\partial x_i}\left(\phi\langle\alpha_f\zeta n_i\delta_w\rangle_f\frac{\langle\overline{\Phi}\delta_w\rangle_f}{(\rho c_p)_f}\right)}_{(d)}.\end{aligned} \tag{41}$$

Term (a) in Eq. (41) involves the average of the product of the first mapping variable times the velocity fluctuation. It is typical of a dispersion term, and, in our particular case, it should be referred to as "passive dispersion" since it is

equivalent to the one found in the dispersion problem for a passive scalar [4]. The contribution (b) is also a part of the dispersion phenomenon. It appears as a transport term of the mean thermal source term, with a transport coefficient equal to $\langle \delta\overline{u_i}\zeta\rangle_f$. It shall be referred to as "active dispersion" since it is related to the exchange with the other phase. The tortuosity is modeled by the terms (c) and (d). In the same way as for dispersion, term (c) is equivalent to the one encountered in the classical passive scalar study. On the contrary, term (d) is an additional term accounting for the heat source term.

Let us notice that from closure relation (29), one can deduce a rather complex decomposition (with additional contributions) for the macroscopic turbulent diffusion. Doing so, one could avoid definition (16) without modifying the local closure problem.

6. Dimensionless formulation of the closure problem

Several notations are introduced in order to get dimensionless equations. In porous media analysis, the interfacial specific area $\langle\delta_w\rangle_f$ may be defined by

$$\langle\delta_w\rangle_f = \frac{A_f \cap \Delta V}{\Delta V_f}, \tag{42}$$

where the $\cap$ symbol denotes the intersection between two spatial domains. For thermal hydraulic applications, we prefer to use the hydraulic diameter concept. We recall that D_H is proportional to the ratio between the wetted perimeter P_w and the flow area S_w,

$$D_H = 4S_w/P_w. \tag{43}$$

However, for stratified media, D_H is equivalent to $\langle\delta_w\rangle_f$

$$\langle\delta_w\rangle_f = 4/D_H. \tag{44}$$

The bulk flow velocity $\langle\bar{u}\rangle_f = \sqrt{\langle\overline{u_i}\rangle_f\langle\overline{u_i}\rangle_f}$, the thermal diffusivity α_f and the hydraulic diameter D_H are used to build the following macroscopic Péclet number

$$Pe \equiv \frac{\langle\bar{u}\rangle_f D_H}{\alpha_f}. \tag{45}$$

We define an arbitrary reference temperature T_f^r and we also recall the definition of the characteristic diffusion time scale τ_d

$$\tau_d = D_H^2/\alpha_f. \tag{46}$$

Dimensionless variables are denoted with an asterisk

$$\begin{aligned}
&\overline{T_f}^* = \frac{\overline{T_f}}{T_f^r}, \quad t^* = \frac{t}{\tau_d}, \quad \overline{u_i}^* = \frac{\overline{u_i}}{\langle\bar{u}\rangle_f}, \quad \alpha_f^* = \frac{\alpha_f}{\alpha_f} = 1,\\
&\alpha_t^* = \frac{\alpha_t}{\alpha_f}, \quad \alpha_{t_M}^* = \frac{\alpha_{t_M}}{\alpha_f}, \quad x_i^* = \frac{x_i}{D_H}, \quad \delta_w^* = \delta_w D_H,\\
&(\rho c_p)_f^* = \frac{(\rho c_p)_f}{(\rho c_p)_f} = 1, \quad \overline{\Phi}^* = \overline{\Phi}\frac{D_H}{\alpha_f T_f^r}, \quad \eta_j^* = \frac{\eta_j}{D_H},\\
&\zeta^* = \frac{\zeta}{D_H^2/\alpha_f}.
\end{aligned} \tag{47}$$

where α_t^* and $\alpha_{t_M}^*$ are respectively the dimensionless microscopic and macroscopic turbulent thermal diffusivities. The closure relation (29) is written in a dimensionless way

$$\delta\overline{T_f}^* = \eta_i^*\frac{\partial\langle\overline{T_f}^*\rangle_f}{\partial x_i^*} + \zeta^*\langle\overline{\Phi}^*\delta_w^*\rangle_f. \tag{48}$$

We also define the dispersion coefficients

$$\mathscr{D}_{ij}^P = -\langle\delta\overline{u_i}\eta_j\rangle_f, \tag{49}$$

$$\mathscr{D}_i^A = -\langle\delta\overline{u_i}\zeta\rangle_f \tag{50}$$

and the tortuosity coefficients

$$\mathscr{T}_{ij}^P = \langle\eta_j n_i\delta_w\rangle_f, \tag{51}$$

$$\mathscr{T}_i^A = \langle\zeta n_i\delta_w\rangle_f. \tag{52}$$

We choose to scale the dispersion coefficient (49) with the fluid thermal diffusivity

$$\mathscr{D}_{ij}^P = \alpha_f\mathscr{D}_{ij}^{P*} = -\langle\bar{u}\rangle_f D_H\langle\delta\overline{u_i}^*\eta_j^*\rangle_f. \tag{53}$$

The second contribution (50) of the dispersion is homogeneous to a length. We scale it with the hydraulic diameter in order to get

$$\mathscr{D}_i^A = D_H\mathscr{D}_i^{A*} = PeD_H\langle\delta\overline{u_i}^*\zeta^*\rangle_f. \tag{54}$$

Moreover, the dimensional analysis of the tortuosity coefficients leads to

$$\mathscr{T}_{ij}^P = \mathscr{T}_{ij}^{P*} = \langle\eta_j^*\, n_i\delta_w^*\rangle_f, \tag{55}$$

$$\mathscr{T}_i^A = \frac{\mathscr{T}_i^{A*}}{\langle\bar{u}\rangle_f} = \frac{D_H}{\alpha_f}\langle\zeta^*\, n_i\delta_w^*\rangle_f. \tag{56}$$

With these definitions, the macroscopic mean temperature equation reads

$$\begin{aligned}
&\phi\frac{\partial\langle\overline{T_f}^*\rangle_f}{\partial t^*} + \frac{\partial\phi Pe\langle\overline{u_i}^*\rangle_f\,\langle\overline{T_f}^*\rangle_f}{\partial x_i^*}\\
&\quad= \frac{\partial}{\partial x_i^*}\left[\phi(1+\alpha_{t_M}^*)\frac{\partial\langle\overline{T_f}^*\rangle_f}{\partial x_i^*}\right] + \phi\langle\overline{\Phi}^*\delta_w^*\rangle_f\\
&\qquad+ \frac{\partial}{\partial x_i^*}\left(\phi\mathscr{D}_{ij}^{P*}\frac{\partial\langle\overline{T_f}^*\rangle_f}{\partial x_j^*}\right) + \frac{\partial}{\partial x_i^*}\left(\phi\mathscr{D}_i^{A*}\langle\overline{\Phi}^*\delta_w^*\rangle_f\right)\\
&\qquad+ \frac{\partial}{\partial x_i^*}\left(\phi\mathscr{T}_{ij}^{P*}\frac{\partial\langle\overline{T_f}^*\rangle_f}{\partial x_j^*}\right) + \frac{\partial}{\partial x_i^*}\left(\phi Pe^{-1}\mathscr{T}_i^{A*}\langle\overline{\Phi}^*\delta_w^*\rangle_f\right).
\end{aligned} \tag{57}$$

In the same way, the closure problem can be rewritten in a dimensionless way

inside the REV:
$$Pe\overline{u_i}^*\frac{\partial\eta_j^*}{\partial x_i^*}-\frac{\partial}{\partial x_i^*}\left[\left(1+\alpha_t^*\right)\frac{\partial\eta_j^*}{\partial x_i^*}\right]=\left(\frac{\partial\alpha_t^*}{\partial x_j^*}-Pe\delta\overline{u_j}^*\right), \tag{58}$$

$$Pe\overline{u_i}^*\frac{\partial\zeta^*}{\partial x_i^*}-\frac{\partial}{\partial x_i^*}\left[\left(1+\alpha_t^*\right)\frac{\partial\zeta^*}{\partial x_i^*}\right]=-1, \tag{59}$$

on A_f:
$$\frac{\partial\eta_j^*}{\partial x_i^*}=-\delta_{ij}, \tag{60}$$

$$\frac{\partial\zeta^*}{\partial x_i^*}n_i=\frac{\overline{\Phi}^*}{\langle\overline{\Phi}^*\delta_w^*\rangle_f}, \tag{61}$$

periodicity:
$$\eta_j^*(\mathbf{x}^*+p_i^*)=\eta_j(\mathbf{x}^*),\zeta^*(\mathbf{x}^*+p_i^*)=\zeta^*(\mathbf{x}^*), \tag{62}$$

additional relation:
$$\langle\eta_j^*\rangle_f\frac{\partial\langle\overline{T_f}^*\rangle_f}{\partial x_j^*}+\langle\zeta^*\rangle_f\langle\overline{\Phi}^*\delta_w^*\rangle_f=0. \tag{63}$$

7. Application to a plate heat exchanger: laminar flow

In this section, we consider a steady flow passing through a flat plate heat exchanger (see Fig. 2). This system is periodic and made by infinite parallel plates. Heat transfer between the fluid and solids occurs only at the walls. The characteristic length-scale evolution is assumed to be large, such that

$\langle\overline{\Phi}^*\rangle_f\simeq\overline{\Phi}^*$ and consequently (see Eq. (44)):
$$\langle\overline{\Phi}^*\delta_w^*\rangle_f\simeq\langle\delta_w^*\rangle_f\overline{\Phi}^*=4\overline{\Phi}^*. \tag{64}$$

We recall that, for laminar flows, there is no need to use the statistical average operator since statistical fluctuations are zero in this case. Nevertheless, in order to remain consistent with notations used in the other sections, we maintain the statistical average operator in the equations. In the geometry under study, the microscopic temperature profile is symmetrical so that, due to (29), profiles of η and ζ are also symmetric. The tortuosity is related to wall normals. In such a geometry, the tortuosity contributions are zero. The one-dimensional macroscopic temperature equation then reads

$$\underbrace{Pe\frac{\partial\langle\overline{T_f}^*\rangle_f}{\partial z^*}}_{\text{convection}}=\underbrace{\frac{\partial^2\langle\overline{T_f}^*\rangle_f}{\partial z^{*2}}}_{\text{molecular diffusion}}+\underbrace{4\overline{\Phi}^*}_{\text{wall heat flux contribution}}+\underbrace{\frac{\partial}{\partial z^*}\left(\mathscr{D}_{zz}^{P*}\frac{\partial\langle\overline{T_f}^*\rangle_f}{\partial z^*}\right)}_{\text{passive dispersion contribution}}+\underbrace{\frac{\partial}{\partial z^*}\left[\mathscr{D}_z^{A*}\times4\overline{\Phi}^*\right]}_{\text{thermal active dispersion contribution}}. \tag{65}$$

The dispersion coefficients can be deduced from the analysis of the statistically averaged microscopic flow by using the closure problems (58)–(63). The separation of scales allows one to consider that the macroscopic evolution is a succession of equilibrium states (equivalent to z-periodic flow within the REV) at the statistically averaged microscopic scale. Macroscopic quantities are supposed constant inside a REV, in particular, the macroscopic

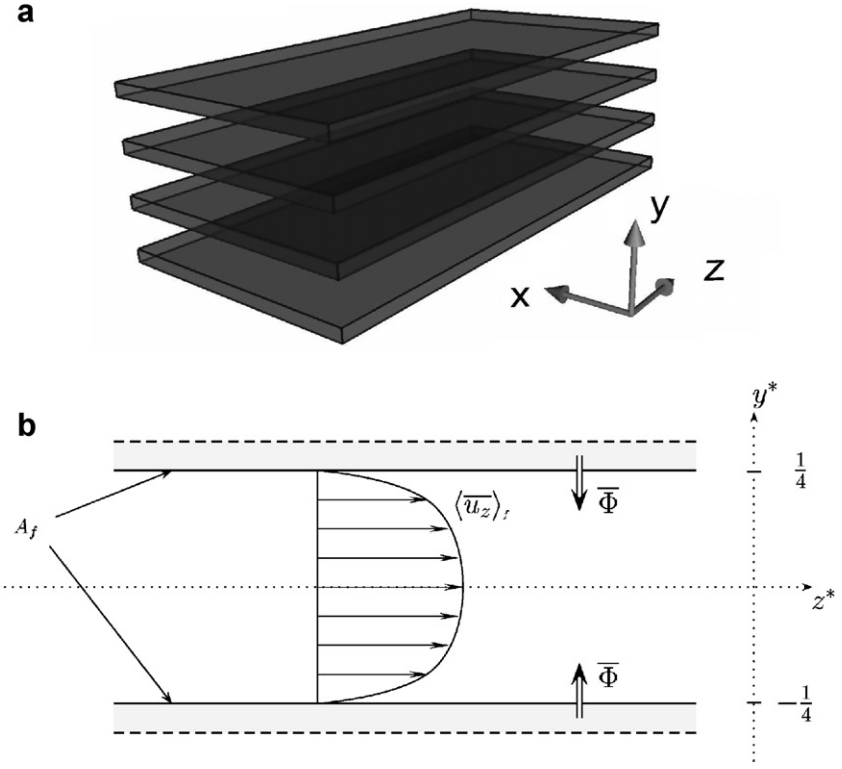

Fig. 2. Description of the stratified porous media under study. The hydraulic diameter is twice the clearance between two successive heating plates. Each dotted line represents a symmetry plane. (a) Tridimensional sketch of a stratified porous media composed of flat plane channels. (b) Bidimensional sketch of one flat plane channel.

temperature gradient and the volume averaged heat flux. Within the REV, velocity and temperature deviation profiles are self-similar and the flow is homogeneous in the z-direction. In such a configuration, the closure relationship (48) gives

$$\delta\overline{T_{\mathrm{f}}}^{*}(y) = \eta_z^*(y^*)\frac{\partial\langle\overline{T_{\mathrm{f}}}^{*}\rangle_{\mathrm{f}}}{\partial z^*} + \zeta^*(y^*)\times 4\overline{\Phi}^* \tag{66}$$

within the REV. In addition, the dimensionless laminar velocity field between two infinite plates is given by

$$\overline{u_z}^*(y) = \frac{3}{2} - 24y^{*2}. \tag{67}$$

The closure problem is considerably simplified thanks to the geometry of the channel

$$\text{inside the REV:}\quad \frac{\partial^2\eta_z^*}{\partial y^{*2}} = Pe\left(\frac{1}{2} - 24y^{*2}\right), \tag{68}$$

$$\frac{\partial^2\zeta^*}{\partial y^{*2}} = 1, \tag{69}$$

$$\text{on } A_{\mathrm{f}}:\quad \frac{\partial\eta_z^*}{\partial y^*}n_y = 0, \tag{70}$$

$$\frac{\partial\zeta^*}{\partial y^*}n_y = \frac{1}{4}, \tag{71}$$

$$\text{periodicity:}\quad \eta_z^*(\mathbf{x}^* + l_z^*) = \eta_z(\mathbf{x}^*),$$

$$\zeta^*(\mathbf{x}^* + l_z^*) = \zeta(\mathbf{x}^*), \tag{72}$$

$$\text{additional relation:}\quad \langle\eta_z^*\rangle_{\mathrm{f}}\frac{\partial\langle\overline{T_{\mathrm{f}}}^{*}\rangle_{\mathrm{f}}}{\partial z^*} + 4\overline{\Phi}^*\langle\zeta^*\rangle_{\mathrm{f}} = 0. \tag{73}$$

The dispersion functions that satisfy this system can easily be found analytically. We obtain

$$\eta_z^*(y) = Pe\left(\frac{y^{*2}}{4} - 2y^{*4} - \frac{1}{128}\right) + C_\eta, \tag{74}$$

$$\zeta^*(y) = \left(\frac{y^{*2}}{2} - \frac{1}{32}\right) + C_\zeta. \tag{75}$$

The constants C_η and C_ζ depend on the wall temperature, but their determination is not necessary to calculate the dispersion coefficients because their contributions are zero, once multiplied by the velocity deviation and spatially averaged over the REV. In general, the values of these constants only act on tortuosity. The additional relation (40) (or Eq. (63) in the dimensionless study) allows one to determine a relation between both constants.

The modeled temperature deviation, described by Eq. (66), corresponds to the exact solution of the temperature deviation obtained from the local energy Eq. (9) with temperature time derivative equal to zero

$$\delta\overline{T_{\mathrm{f}}}^{*} = 4\overline{\Phi}^*\left(\frac{3}{4}y^{*2} - 2y^{*4} - \frac{5}{128}\right) + \left(\overline{T_{\mathrm{w}}}^{*} - \langle\overline{T_{\mathrm{f}}}^{*}\rangle_{\mathrm{f}}\right). \tag{76}$$

In fact, each simplification used to derive the closure problems is *exact* for the flat plane channel flow. Finally, both effective dispersion coefficients can be determined by averaging the products $\eta_z^*\delta\overline{u_z^*}$ and $\zeta^*\delta\overline{u_z^*}$ over the REV

$$\mathscr{D}_{zz}^{P*} = -Pe\langle\eta_z^*\delta\overline{u_z}^{*}\rangle_{\mathrm{f}} = \frac{Pe^2}{840}, \tag{77}$$

$$\mathscr{D}_{z}^{A*} = -Pe\langle\zeta^*\delta\overline{u_z}^{*}\rangle_{\mathrm{f}} = \frac{Pe}{240}. \tag{78}$$

The first result is equivalent (note a coefficient of 840 instead of 210 due to a difference in the choice of the reference length) to the one that can be obtained by applying Taylor–Aris theory to the stratified case (see [19]).

8. Application to a plate heat exchanger: turbulent flows

In this section, we present results for fully developed turbulent flows in flat plate heat exchangers. We evaluate and compare the various macroscopic fluxes, such as the dispersive and diffusive ones. The solution of the closure problem for laminar flows exhibits a quadratic dependence of $\mathscr{D}_{zz}^{P*}$ on the Péclet number. For Poiseuille laminar flows, the velocity profile is self-similar. On the contrary, once the flow becomes turbulent, the velocity profile depends on the turbulence intensity: the microscopic quantities cannot be calculated analytically. For turbulent flows in pipes, Taylor [8] described the velocity profile with an experimental law and the turbulent viscosity with a simple law which is equivalent to a mixing length closure. These descriptions allowed him to show the dependency of the passive dispersion coefficient with the Péclet number of the flow and the friction coefficient

$$\mathscr{D}_{zz}^{P*} \propto Pe\sqrt{f_{\mathrm{p}}}. \tag{79}$$

We underline that for channel flows (which gather both pipe and plane channel flows) the friction coefficient is related to the friction velocity and the bulk velocity

$$f_{\mathrm{p}} = 8\frac{u_{\mathrm{f}}^2}{\langle\bar{u}_z\rangle_{\mathrm{f}}^2}. \tag{80}$$

In our analysis, in order to approach the mean velocity profile between two plates, we have chosen to implement the k–ε model proposed by Chien [20]. The equations of the model are

$$\frac{\partial k}{\partial t} + \overline{u_i}\frac{\partial k}{\partial x_i} = \nu_{\mathrm{t}}\frac{\partial\overline{u_i}}{\partial x_j}\frac{\partial\overline{u_i}}{\partial x_j} + \frac{\partial}{\partial x_j}\left[\left(\nu + \frac{\nu_{\mathrm{t}}}{\sigma_k}\right)\frac{\partial k}{\partial x_j}\right] - \epsilon - \epsilon_{\mathrm{p}}, \tag{81}$$

$$\frac{\partial\epsilon}{\partial t} + \overline{u_i}\frac{\partial\epsilon}{\partial x_i} = \nu_{\mathrm{t}}C_{\epsilon_1}\frac{\epsilon}{k}\frac{\partial\overline{u_i}}{\partial x_j}\frac{\partial\overline{u_i}}{\partial x_j} + \frac{\partial}{\partial x_j}\left[\left(\nu + \frac{\nu_{\mathrm{t}}}{\sigma_\epsilon}\right)\frac{\partial\epsilon}{\partial x_j}\right] - C_{\epsilon_2}f_2\frac{\epsilon^2}{k} + E_{\mathrm{p}}, \tag{82}$$

where the turbulent kinematic viscosity is defined by

$$\nu_{\mathrm{t}} = C_\mu f_\mu\frac{k^2}{\epsilon}. \tag{83}$$

The wall functions ϵ_{p} and E_{p} allow the model to simulate the turbulence behavior in the channel flow. The coefficients used in this paper are given below

$$C_\mu = 0.09,\quad C_{\epsilon_1} = 1.44,\quad C_{\epsilon_2} = 1.92,\quad \sigma_k = 1,$$
$$\sigma_\varepsilon = 1.3. \tag{84}$$

One can notice that, for the configuration under study, the axial turbulent diffusivity gradient is zero. Its influence only

acts on flows such as those encountered in really multidimensional configurations, for example transverse flows in rod bundles. Moreover, the turbulent treatment in wall shear flows may be achieved by various ways. Specific low-Reynolds number models have already been developed, relating for instance α_t to k, ε, the temperature fluctuation covariance and the turbulent thermal dissipation (see [21]). The use of such models requires the introduction of damping functions into the closure problem. Since our goal is to maintain a simplified description of the statistically averaged microscopic flow, this solution cannot be adopted here. Our goal is also to maintain the possibility to use the development presented in this paper for other flow quantities than temperature [14], for instance concentration. Therefore the dispersion problem should remain as general as possible. Thus, a practical alternative is to consider a dependence between the momentum and the temperature turbulent transports, introducing the turbulent Prandtl number

$$Pr_t = \frac{\nu_t}{\alpha_t}. \tag{85}$$

This parameter can be defined as a simple constant or as a function of the distance to the wall. For simple geometries such as those considered in this paper and for water flows, $Pr_t = 0.9$ seems a reasonable choice [22].

The flow is assumed to be fully turbulent for Reynolds numbers, based on the hydraulic diameter, higher than 4000. Hence, the Reynolds number values are taken in the range about 4×10^3 to 10^7. A Gaussian mesh, made of 300 grid points, is used. All normalized residuals are brought down to 10^{-4}. One can see in Fig. 3a that the normalized velocity profile $u^+ = \bar{u}_z/u_f$ exhibits the expected linear behavior in the inner boundary layer. Simulation results also match the Reichardt law given by [23,24]

$$F_u(y^+) = u^+ = \frac{1}{0.41}\ln(1+0.41y^+) + 7.8\left(1-\exp\left(-\frac{y^+}{11}\right)-\frac{y^+}{11}\exp\left(-\frac{y^+}{3}\right)\right). \tag{86}$$

The resulting simulated fields are then used to numerically solve the following closure problem

$$\text{inside the REV:}\quad \frac{\partial}{\partial y^*}\left[(1+\alpha_t^*)\frac{\partial \eta_z^*}{\partial y^*}\right] = Pe\delta\overline{u_z}^*, \tag{87}$$

$$\frac{\partial}{\partial y^*}\left[(1+\alpha_t^*)\frac{\partial \zeta^*}{\partial y^*}\right] = 1, \tag{88}$$

$$\text{on } A_f:\quad \frac{\partial \eta_z^*}{\partial y^*}n_y = 0, \tag{89}$$

$$\frac{\partial \zeta^*}{\partial y^*}n_y = \frac{1}{4}, \tag{90}$$

$$\text{periodicity:}\quad \eta_z^*(\mathbf{x}^* + l_z^*) = \eta_z(\mathbf{x}^*),\quad \zeta^*(\mathbf{x}^* + l_z^*) = \zeta(\mathbf{x}^*), \tag{91}$$

$$\text{additional relation:}\quad \langle \eta_z^* \rangle_f \frac{\partial \langle \overline{T}_f^* \rangle_f}{\partial z^*} + 4\overline{\Phi}^* \langle \zeta^* \rangle_f = 0. \tag{92}$$

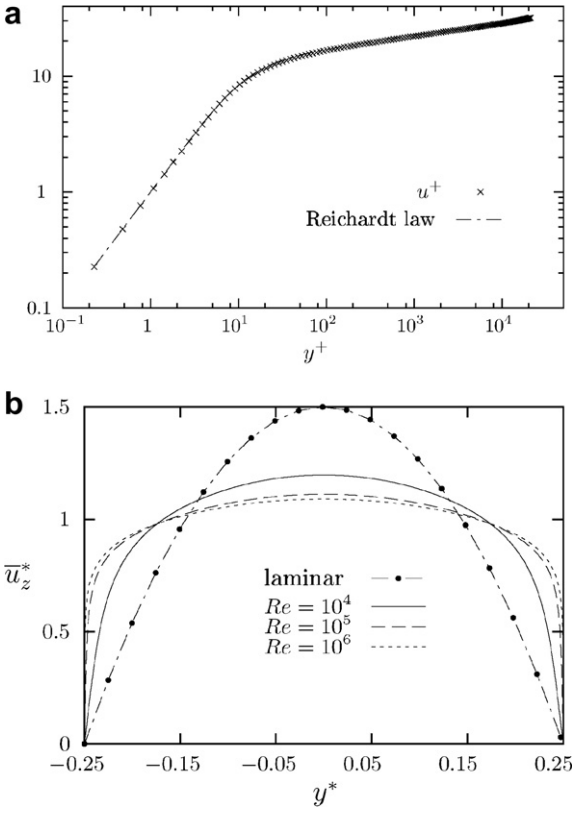

Fig. 3. Description and validation of the velocity profiles for a flat plate channel flow. (a) Velocity profile in the boundary layer. Both the log-profile in the turbulent boundary layer and the linear profile in the viscous sublayer are well recovered by our calculations. $Re = 5 \times 10^6$. (b) Dimensionless turbulent velocity profiles for different Reynolds numbers. For small Reynolds numbers ($Re \sim 10^4$) the turbulent boundary layer strongly affects the bulk flow velocity profile. The boundary layer thickness evolves significantly from $Re = 10^4$ to $Re = 10^5$. For $Re > 10^5$, the boundary layer thickness does not evolve significantly: the thickness of the defect region becomes dominant.

Except the macroscopic turbulent diffusion term, the macroscopic balance equation of the spatially averaged fluid temperature is similar as in the laminar case:

$$\underbrace{Pe\frac{\partial \langle \overline{T}_f^* \rangle_f}{\partial z^*}}_{\text{convection}} = \underbrace{\frac{\partial}{\partial z^*}\left((1+\alpha_{t_M}^*)\frac{\partial \langle \overline{T}_f^* \rangle_f}{\partial z^*}\right)}_{\text{molecular and turbulent diffusion}} + \underbrace{4\overline{\Phi}^*}_{\text{wall heat flux contribution}} + \underbrace{\frac{\partial}{\partial z^*}\left(\mathscr{D}_{zz}^{P*}\frac{\partial \langle \overline{T}_f^* \rangle_f}{\partial z^*}\right)}_{\text{passive dispersion contribution}} + \underbrace{\frac{\partial}{\partial z^*}\left[4\overline{\Phi}^*\mathscr{D}_z^{A*}\right]}_{\text{thermal active dispersion contribution}}. \tag{93}$$

The various fluxes, i.e., diffusive, passive dispersive and active dispersive fluxes, will be compared. Their expressions are

$$\text{diffusive flux:}\quad (1+\alpha_{t_M}^*)\frac{\partial \langle \overline{T}_f^* \rangle_f}{\partial z^*}, \tag{94}$$

$$\text{passive dispersive flux:}\quad \mathscr{D}_{zz}^{P*}\frac{\partial \langle \overline{T}_f^* \rangle_f}{\partial z^*}, \tag{95}$$

$$\text{active dispersive flux:}\quad 4\overline{\Phi}^*\mathscr{D}_z^{A*}. \tag{96}$$

Thanks to system (87), (89)–(92), an analysis of the η_z^* and ζ^* evolution can be carried out.

We recall that, in the simple configuration under study, the equation for η_z^* has a sole source term for both laminar and turbulent regimes: the velocity deviation. However for a given geometry and within the laminar regime, the velocity shape is self-similar and its magnitude is given by the Reynolds number. The temperature profile is modulated by the Prandtl number. We can then argue that, within the laminar regime, the function $\mathscr{D}_{zz}^{P*}$ only depends on the Péclet number, the definition of which is

$$Pe = RePr. \tag{97}$$

On the contrary, for a steady turbulent flow in a given geometry, even the shape of the dimensionless velocity profile is related to the Reynolds number. Furthermore, with the adopted first gradient closure for the turbulent heat flux, the temperature profile depends upon two additional quantities: the Prandtl and the turbulent Prandtl numbers. From the boundary layer theory [25,26], the ratio between the conductive and the viscous sublayer thickness can be estimated by

$$\frac{\delta_t}{\delta_v} \propto \frac{1}{\sqrt{Pr}}. \tag{98}$$

For Reynolds numbers ranging from the turbulent transition value to few 10^4, the boundary layer thickness is of the same order of magnitude than the thickness of the defect zone. In this range, the Prandtl number strongly influences the temperature profile. Hence, the temperature profile in the turbulent regime cannot only be scaled by Pe since Pr and Re are intrinsically independent variables.

Nevertheless, for Reynolds numbers higher than 10^5, the boundary layer thickness becomes negligible with respect to the defect zone, and the Prandtl number does not affect the temperature profile significantly (if $Pr \sim 1$). It gives only an indication of the α_t magnitude . The velocity profile does not significantly evolve while the Reynolds number increases (see Fig. 3b), except in the boundary layer where the velocity profile is tightly related to the friction coefficient (Eq. (86)).

Once the η_z^* function is determined, the $\mathscr{D}_{zz}^{P*}$ coefficient can be calculated by volume averaging the product $\eta_z^* \delta\overline{u_z}^*$ and multiplying the result by the Péclet number. From Fig. 4, one can notice the separation between the laminar solution and the turbulent solution. Indeed, no attempt of connection between these two types of solutions is carried out in this paper. The gap between both regimes depends on the Prandtl number. This is induced by a variable conductive sublayer thickness. Then, for Reynolds numbers ranging from 4×10^3 to 10^5, the two different Prandtl number simulations, represented in Fig. 4, exhibit slightly different behaviors, as inferred above. But, for highly turbulent flow, say $Re > 10^5$, the averaged product $\langle \eta_z^* \delta\overline{u_z}^* \rangle_f$ remains nearly constant. We recall here that dispersion only occurs if the velocity profile is non-uniform. The transition from Pe^2 dependence in the laminar regime

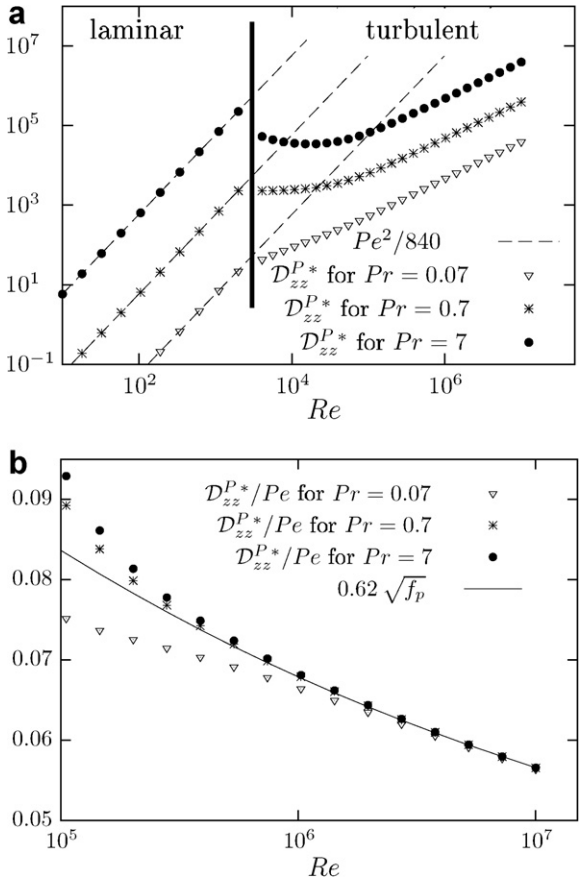

Fig. 4. Laminar and turbulent plane channel flow: study of the passive dispersion coefficient $\mathscr{D}_{zz}^{P*}$. Three Prandtl number flows have been simulated. (a) Evolution of $\mathscr{D}_{zz}^{P*}$ with the Reynolds number. (b) Evolution of $\mathscr{D}_{zz}^{P*}/\mathscr{P}_e$.

to a close-to-Pe dependence in the strong turbulent regime is induced by a flatter velocity profile in the main part of the "pore".

Due to Eq. (77), the product $\langle \eta_z^* \delta\overline{u_z}^* \rangle_f$ is equal to the ratio $\mathscr{D}_{zz}^{P*}$ and, according to Taylor's analysis, this ratio is a function of the square root of the friction coefficient (Eq. (80)). Thanks to an optimisation on results corresponding to Reynolds numbers higher than 5×10^5, our results agree with this former analysis and we get (see Fig. 4b)

$$\text{for } Re > 5 \times 10^5, \quad \frac{\mathscr{D}_{zz}^{P*}}{Pe} = \mathscr{C}_p \sqrt{f_p}, \tag{99}$$

where

$$\mathscr{C}_p \simeq 0.62. \tag{100}$$

The friction coefficient dependency of the passive dispersion coefficient is induced by the term in the right hand side of the closure Eq. (87), which is equal to the velocity deviation.

Eq. (88) for ζ^* has one source term equal to 1. The diffusion term of Eq. (88) is also related to the turbulent thermal diffusivity. Hence, the dispersion function is intrinsically related to Re, Pr and Pr_t. According to (78), the

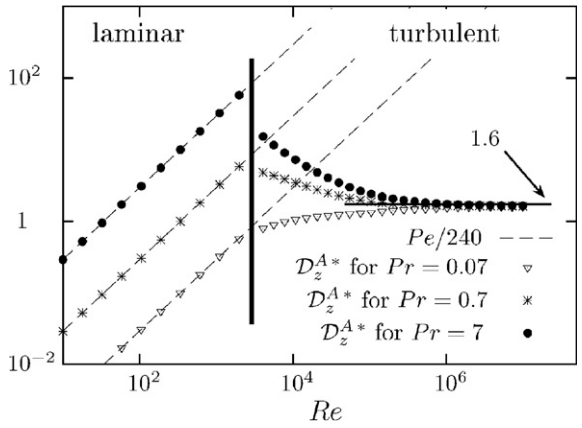

Fig. 5. Laminar and turbulent plane channel flow: study of the active dispersion coefficient $\mathscr{D}_z^{A*}$. Our calculations match the analytical results in the laminar regime. For turbulent flows, the dispersion coefficient $\mathscr{D}_z^{A*}$ achieves a constant value close to 1.6 as the Reynolds number increases.

coefficient $\mathscr{D}_z^{A*}$ is calculated by averaging the product $\zeta^* \delta\overline{u_z}^*$ and by multiplying it with the Péclet number. Whereas the product $\zeta^* \delta\overline{u_z}^*$ is constant within the laminar regime, it decreases as the Reynolds number or the Prandtl number increases because of the turbulent thermal diffusivity action in the ζ^* equation (Fig. 5). For Re greater than 10^5, the coefficient $\mathscr{D}_z^{A*}$ asymptotically achieves a constant value

$$\mathscr{D}_z^{A*} = \mathscr{C}_A, \tag{101}$$

where $\mathscr{C}_A$ is given by

$$\mathscr{C}_A \simeq 1.6. \tag{102}$$

9. Application to a plate heat exchanger: comparison between dispersion and diffusion

We now want to compare the dispersion and diffusion contributions in the balance Eq. (93) for the macroscopic fluid temperature. Note that this equation is verified even for turbulent or laminar flows by setting $\alpha_{t_M}^*$ to zero when the Reynolds number is lower than 2×10^3.

Furthermore, due to the homogeneity along the z axis within the REV, the derivatives of the dispersive and diffusive contributions are zero. Removing these terms from relation (93), an estimation of the macroscopic temperature gradient within the REV can be given by

$$Pe \frac{\partial \langle \overline{T_f}^* \rangle_f}{\partial z^*} \simeq 4\overline{\Phi}^*. \tag{103}$$

This result supports the remark done in Section 4 concerning the leading role of the macroscopic temperature gradient and the fact that it cannot be neglected. Nevertheless, the dispersive and the diffusive fluxes are not zero. They read in a dimensionless way

$$\text{diffusive flux: } (1 + \alpha_{t_M}^*) \frac{\partial \langle \overline{T_f}^* \rangle_f}{\partial z^*}, \tag{104}$$

$$\text{passive dispersive flux: } \mathscr{D}_{zz}^{P*} \frac{\partial \langle \overline{T_f}^* \rangle_f}{\partial z^*}, \tag{105}$$

$$\text{active dispersive flux: } \mathscr{D}_z^{A*} \times 4\overline{\Phi}^* = Pe \mathscr{D}_z^{A*} \frac{\partial \langle \overline{T_f}^* \rangle_f}{\partial z^*}. \tag{106}$$

Within the laminar regime, we use the results (77) and (78) to compare the various fluxes

$$\frac{\text{passive dispersive flux}}{\text{diffusive flux}} = \frac{\mathscr{D}_{zz}^{P*}}{1} = \frac{Pe^2}{840}, \tag{107}$$

$$\frac{\text{active dispersive flux}}{\text{diffusive flux}} = \frac{Pe \mathscr{D}_z^{A*}}{1} = \frac{Pe^2}{240}, \tag{108}$$

$$\frac{\text{active dispersive flux}}{\text{passive dispersive flux}} = \frac{Pe \mathscr{D}_z^{A*}}{\mathscr{D}_{zz}^{P*}} = \frac{7}{2}. \tag{109}$$

From these we see that each "dispersion" flux contribution rapidly predominates over the molecular diffusive flux for increasing Péclet numbers. Furthermore, the ratio between active dispersion and passive dispersion is equal to 3.5.

Now, within the turbulent regime, no model for the macroscopic turbulent diffusivity has been developed in this work. Nevertheless, due to the α_{t_M} definition, Eq. (16), and the self-similar hypothesis within the REV, we have in a dimensionless way

$$\left\langle \alpha_t^* \frac{\partial \overline{T_f}^*}{\partial x_i^*} \right\rangle_f = \langle \alpha_t^* \rangle_f \frac{\partial \langle \overline{T_f}^* \rangle_f}{\partial x_i^*} = \alpha_{t_M}^* \frac{\partial \langle \overline{T_f}^* \rangle_f}{\partial x_i^*}. \tag{110}$$

Using the Prandtl number definition and the turbulent Prandtl number definition, Eq. (85), we deduce that, within the REV,

$$\alpha_{t_M}^* = \langle \alpha_t^* \rangle_f = \langle \nu_t \rangle_f \frac{Pr}{Pr_t}. \tag{111}$$

Taylor's analysis [8], briefly introduced in Section 8, suggests that the spatially averaged turbulent viscosity is related to the square root of the friction factor. Fig. 6 allows us to qualitatively show the same result, using a more elaborated turbulence model and for Reynolds numbers higher than 10^5. We thus get

$$\langle \nu_t^* \rangle_f \simeq \mathscr{C}_\nu Re \sqrt{f_p}. \tag{112}$$

where

$$\mathscr{C}_\nu \simeq 6.62 \times 10^{-3}. \tag{113}$$

Using (99) and (111), for Reynolds numbers higher than 5×10^5, the ratio between the passive dispersive flux and the effective diffusive flux reads

$$\frac{\text{passive dispersive flux}}{\text{diffusive flux}} = \frac{\mathscr{D}_{zz}^{P*}}{1 + \langle \alpha_t^* \rangle_f} = \frac{\mathscr{C}_P Pe \sqrt{f_p}}{1 + \langle \nu_t^* \rangle_f Pr/Pr_t}. \tag{114}$$

For the Reynolds number and Prandtl number values considered in this work, one can notice that $\langle \nu_t^* \rangle_f Pr/Pr_t \gg 1$. Due to Eq. (112), we show

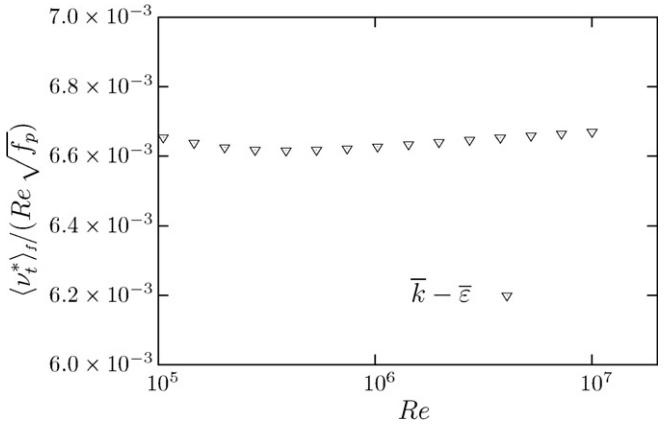

Fig. 6. Turbulent plane channel flow: study of the $\langle v_t^* \rangle_f / (Re\sqrt{f_p})$ with the Reynolds number.

$$\frac{\text{passive dispersive flux}}{\text{diffusive flux}} \simeq \frac{\mathscr{C}_P}{\mathscr{C}_v} Pr_t. \tag{115}$$

Obviously, the value of this ratio is sensitive to the calibration of the turbulence model. In the case under study, with the values selected for the turbulence model and according to values of $\mathscr{C}_P$ and $\mathscr{C}_v$, respectively given by (100) and (113), we obtain

$$\frac{\text{passive dispersive flux}}{\text{diffusive flux}} \simeq 84. \tag{116}$$

This "asymptotic" study is assessed by the simulation results shown in Fig. 7. One can conclude that, for the flat plane channel geometry, the passive dispersive flux rules over the turbulent heat flux in the main stream direction.

In addition, we use the formulation given by (106) to compare the active dispersive flux with the thermal diffusive flux (Fig. 8). In the laminar regime, the ratio of these two fluxes increases quadratically with the Péclet number,

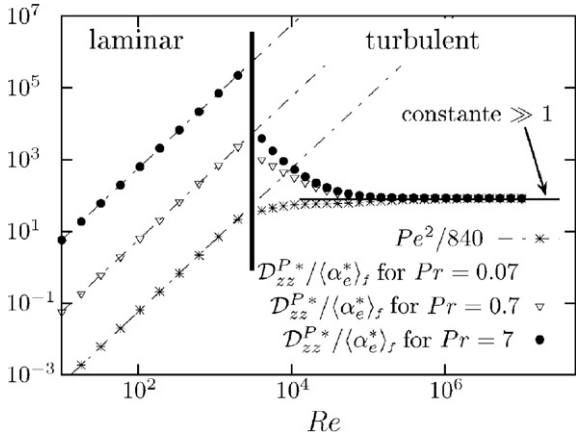

Fig. 7. Laminar and turbulent plane channel flow: comparison between dimensionless axial dispersion and averaged effective thermal diffusivity ($\langle \alpha_e^* \rangle_f = 1 + \langle \alpha_t^* \rangle_f$). Our calculations match the analytical results for the laminar regime. For high Reynolds number flows ($Re > 10^5$), the ratio achieves a constant value much greater than one. This value does not depend on the Prandtl number.

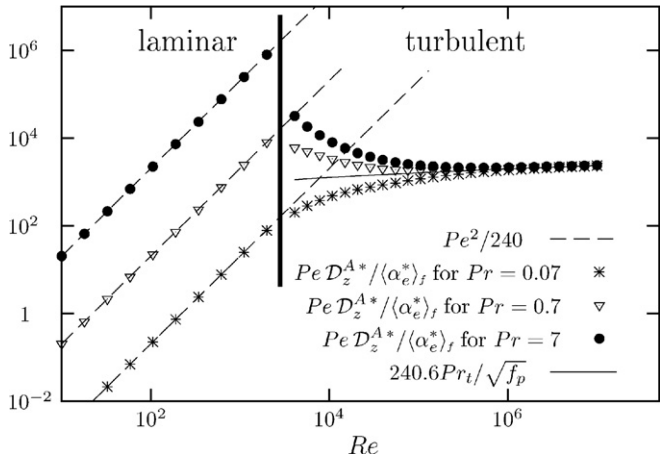

Fig. 8. Laminar and turbulent plane channel flow: study of $(Pe\mathscr{D}_z^{A*})$ scaled with the averaged dimensionless effective thermal diffusivity ($\langle \alpha_e^* \rangle_f = 1 + \langle \alpha_t^* \rangle_f$). Our computations match the analytical results in the laminar regime. For $Re > 10^5$, the ratio slowly increases.

such that this dispersion contribution also rapidly becomes dominant with respect to the thermal diffusion $\langle \alpha_f^* \rangle_f$. This is to be compared with the analytical results presented in Section 7. For Reynolds number greater than few 10^5, we have the asymptotic limits

$$\frac{\text{active dispersive flux}}{\text{diffusive flux}} = \frac{Pe\mathscr{D}_z^{A*}}{1 + \langle \alpha_t^* \rangle_f} = \frac{\mathscr{C}_A Pe}{1 + \langle v_t^* \rangle_f Pr/Pr_t}. \tag{117}$$

As $\langle v_t^* \rangle_f Pr/Pr_t \gg 1$, and due to Eq. (112), we get

$$\frac{\text{active dispersive flux}}{\text{diffusive flux}} = \frac{\mathscr{C}_A}{\mathscr{C}_v} \frac{Pr_t}{\sqrt{f_p}}. \tag{118}$$

Considering the $\mathscr{C}_A$ and $\mathscr{C}_v$ values respectively given by (102) and (113), we show that for Reynolds number values higher than few 10^5

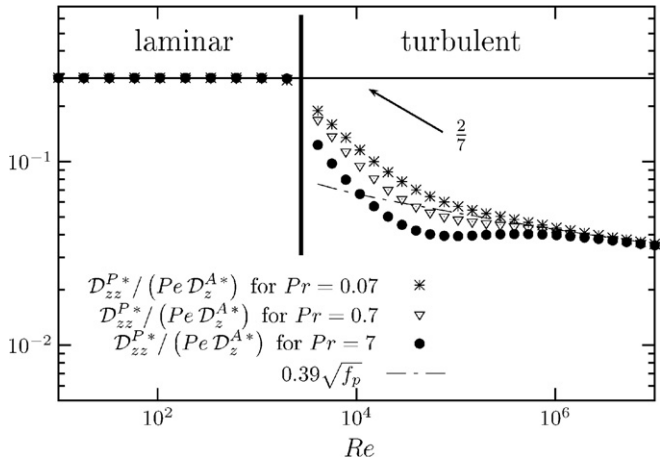

Fig. 9. Comparison between the two dispersion coefficients (under their diffusive form). The active dispersion coefficient is much higher than the ordinary dispersion one in both laminar and turbulent regime. More precisely, $\mathscr{D}_{zz}^{P*}$ is at least one order of magnitude lower than $(Pe\mathscr{D}_z^{A*})$ for $Re > 10^4$.

Table 2
Channel flow study: summary of the results about dispersion within both laminar and turbulent regimes

	Plane channel laminar flow	Tube channel laminar flow	Plane channel asymptotic behavior	Tube channel asymptotic behavior
$\mathscr{D}_{zz}^{P*}$	$Pe^2/840$	$Pe^2/192$	$0.62\sqrt{f_p}Pe$	$0.39\sqrt{f_p}Pe$
$\mathscr{D}_{z}^{A*}$	$Pe/240$	$Pe/96$	1.6	1
$\mathscr{D}_{zz}^{P*}/\langle\alpha_e^*\rangle_f$	$Pe^2/840$	$Pe^2/192$	$93Pr_t$	$24.4Pr_t$
$Pe\mathscr{D}_{z}^{A*}/\langle\alpha_e^*\rangle_f$	$Pe^2/840$	$Pe^2/96$	$240.6Pr_t/\sqrt{f_p}$	$56.25Pr_t/\sqrt{f_p}$
$\mathscr{D}_{zz}^{P*}/(Pe\mathscr{D}_{z}^{A*})$	2/7	1/2	$0.39\sqrt{f_p}$	$0.39\sqrt{f_p}$

$$\frac{\text{active dispersive flux}}{\text{diffusive flux}} = 240.6\frac{Pr_t}{\sqrt{f_p}}. \tag{119}$$

This result is recovered in Fig. 8. We thus underline that the active dispersive flux strongly rules over the effective diffusive flux in the flow direction. The ratio between the two fluxes keeps a slight raising trend for Reynolds number greater than few 10^5.

The active dispersive flux part can also be compared with the passive dispersive flux (Fig. 9). In the laminar regime, the analytical derivation of these two terms exhibits a constant ratio (see Section 7)

$$\frac{\mathscr{D}_{zz}^{P*}}{Pe\mathscr{D}_{z}^{A*}} = \frac{2}{7} \quad (\text{for } Re < 2.10^3). \tag{120}$$

The active dispersive flux is thus greater than the passive dispersive flux. This result is amplified in the turbulent regime. For Reynolds numbers higher than few 10^4, an asymptotic analysis gives an estimation of the ratio $\mathscr{D}_{zz}^{P*}/Pe\mathscr{D}_{z}^{A*}$ for high Reynolds number flows as

$$\frac{\text{passive dispersive flux}}{\text{active dispersive flux}} = \frac{\mathscr{D}_{zz}^{P*}}{Pe\mathscr{D}_{z}^{A*}} = \frac{\mathscr{C}_P}{\mathscr{C}_A}\sqrt{f_p}. \tag{121}$$

According to (100) and (102), this result is equivalent to

$$\frac{\text{passive dispersive flux}}{\text{active dispersive flux}} = 0.39\sqrt{f_p}. \tag{122}$$

The passive dispersive flux is then at least one order of magnitude lower than the active dispersive flux in the flow direction. This result is connected to the strong dependence of the temperature deviation with the thermal source.

In order to have additional results for an other geometry, the same work has been carried out for the tube channel geometry. Results are summarized in Table 2. We underline that trends are qualitatively in agreement for both geometry.

10. Conclusion

In this paper, we have extended the closure problem for thermal dispersion in a porous medium (see for instance [4]) to the turbulent regime in channel flows. To achieve this goal, and following ideas already put forth in the literature, two different averages were used: the statistical and the spatial averages. We choose first to apply the statistical average, with the idea that turbulence length-scale remains smaller than the geometrical characteristic length-scale of the solid structure. The additional turbulent fluxes were modeled through the eddy viscosity concept. This results in a modified closure problem compared to the classical closure problem. In the same way, heat transfer at the walls lead to the introduction of an additional mapping variable in the closure problem, and its evolution equation has been established. The theory is developed in a mixed approach that decouples the solid and fluid phases treatment, following methods used to deal with heat exchangers. This approach splits the up-scaling effects into two different contributions: the first one that accounts for the velocity spatial heterogeneities and the second one that is associated to the wall heat flux. Results with this model have been obtained for channel flows. In the laminar regime, our analytical and numerical calculations agree with the well known Pe^2 dependency of the dispersion coefficient for a passive scalar. The study is then extended to the turbulent regime. The active and passive dispersive fluxes are compared with the thermal diffusive flux. An important conclusion has emerged: both dispersive fluxes rules over the estimated macroscopic turbulent heat flux by at least one order of magnitude in the main flow direction when temperature gradients are governed by wall heat flux. More precisely, for such flows, the active dispersion coefficient is dominant over the macroscopic turbulent thermal diffusion and the passive dispersion coefficient.

Appendix A. Averages

In this appendix, we recall the major results and theorems that are necessary to carry out the developments throughout the paper. We refer the reader to the literature for a review of the various problems and methodological developments [4,27,28]. All properties are presented for simple volume averages, without use of any special weighting functions. For the particular case of periodic structures, the cellular average operator is a relevant tool [27].

A.1. Volume averages and fluid characteristic function

The up-scaling process is linked to the definition of a volume averaging operator which corresponds to a spatial integration over a REV [1] ΔV. For a function ξ, we have

$$\langle\xi\rangle(\mathbf{x},t) \equiv \frac{1}{\Delta V(\mathbf{x})}\int_{\Delta V(\mathbf{x})}\xi(\mathbf{y},t)\mathrm{d}V_{\mathbf{y}}. \tag{A.1}$$

The configuration and the periodicity of the porous medium determines the REV choice. In Eq. (A.1), the REV center point is denoted $\mathbf{x}$, and the notation $\Delta V(\mathbf{x})$ recalls that the averaging volume follows the current point.

We denote χ_f the fluid characteristic function, equal to one in the fluid phase and zero elsewhere. At each point of the solid/fluid interface, we define $\vec{n}$ the normal vector pointing towards the solid phase, and $\vec{\omega}$ the interface velocity. Let δ_w be the Dirac generalized function associated to the interface. Using subscript notations, it is possible to derive the evolution equations for χ_f [29]:

$$\begin{cases} \frac{\partial \chi_f}{\partial t} + \omega_i \frac{\partial \chi_f}{\partial x_i} = 0, \\ \frac{\partial \chi_f}{\partial x_i} = -n_i \delta_w. \end{cases} \tag{A.2}$$

With this definition, the medium porosity is given by

$$\phi = \langle \chi_f \rangle \tag{A.3}$$

and we can introduce the fluid specific average operator (intrinsic average)

$$\langle \xi \rangle_f(\mathbf{x}, t) = \frac{\langle \xi \chi_f \rangle}{\langle \chi_f \rangle} = \frac{1}{\Delta V_f(\mathbf{x})} \int_{\Delta V(\mathbf{x})} \xi(\mathbf{y}, t) \chi_f \, \mathrm{d}V_{\mathbf{y}}, \tag{A.4}$$

where ΔV_f is the volume of fluid contained in the REV. In the same way, calling A_f the interface between fluid and solid phases, one can define the superficial average of a quantity ξ by

$$\langle \xi \delta_w \rangle(\mathbf{x}, t) = \frac{1}{\Delta V(\mathbf{x})} \int_{A_f(\mathbf{x})} \xi(\mathbf{y}, t) \mathrm{d}S_{\mathbf{y}}. \tag{A.5}$$

A.2. Properties of the average operators

In the first place, we introduce the statistical decomposition commonly used for turbulence modeling. Let us consider some turbulent quantity ξ. We assume that this quantity can be written as the sum of its statistical average and a fluctuation

$$\xi = \overline{\xi} + \xi'. \tag{A.6}$$

It is well known that the statistical average (also called Reynolds average) follows the Reynolds axioms. We recall these useful features

$$\begin{array}{ll} \text{Linearity} & \overline{\lambda \xi} = \lambda \overline{\xi}, \text{ where } \lambda \text{ is a constant,} \\ \text{Idempotence} & \overline{\overline{\xi}} = \overline{\xi} \iff \overline{\xi'} = 0, \\ \text{Commutative property with the differential operators} & \left| \begin{array}{l} \overline{\frac{\partial \xi}{\partial t}} = \frac{\partial \overline{\xi}}{\partial t}, \\ \overline{\frac{\partial \xi}{\partial x_i}} = \frac{\partial \overline{\xi}}{\partial x_i}. \end{array} \right. \end{array} \tag{A.7}$$

The same quantity ξ may also be split up into a volumic mean part and a spatial deviation

$$\xi = \langle \xi \rangle_f + \delta\xi. \tag{A.8}$$

The fluid spatial average is clearly linear due to its integral formulation, but does not fulfil the other conditions. Indeed the volume average operator does not commute with the space–time differential operator. Thanks to the derivation rules of the fluid characteristic function (Eq. (A.2)) and to both space and time independence of the REV, the relations usually known as the local volume averaging theorem can be established

$$\begin{aligned} \phi \left\langle \frac{\partial \xi}{\partial x_i} \right\rangle_f &= \left\langle \frac{\partial \xi}{\partial x_i} \chi_f \right\rangle \\ &= \frac{\partial \langle \xi \chi_f \rangle}{\partial x_i} - \left\langle \xi \frac{\partial \chi_f}{\partial x_i} \right\rangle = \frac{\partial \phi \langle \xi \rangle_f}{\partial x_i} + \underbrace{\langle \xi n_i \delta_w \rangle}_{\text{wall contribution}}, \end{aligned} \tag{A.9}$$

$$\begin{aligned} \phi \left\langle \frac{\partial \xi}{\partial t} \right\rangle_f &= \left\langle \frac{\partial \xi}{\partial t} \chi_f \right\rangle \\ &= \frac{\partial \langle \xi \chi_f \rangle}{\partial t} - \left\langle \xi \frac{\partial \chi_f}{\partial t} \right\rangle = \frac{\partial \phi \langle \xi \rangle_f}{\partial t} + \underbrace{\langle \xi \omega_i n_i \delta_w \rangle}_{\text{wall contribution}}. \end{aligned} \tag{A.10}$$

The idempotence of the spatial filter can be assumed if the characteristic length scale of the spatially filtered quantities is large with respect to the characteristic length of the REV [4]. In general, the REV must include numerous pores, but for spatially periodic porous media, it has been shown that effective properties can be calculated with an averaging volume corresponding to the Unit cell [30].

References

[1] M.H.J. Pedras, M.J.S. De Lemos, Macroscopic turbulence modeling for incompressible flow through undeformable porous media, Int. J. Heat Mass Transfer 44 (2001) 1081–1093.

[2] F. Kuwahara, A. Nakayama, H. Koyama, A numerical study of thermal dispersion in porous medium, J. Heat Transfer 118 (1996) 756–761.

[3] G. Taylor, Dispersion of solute matter in solvent flowing slowly through a tube, Proc. Roy. Soc. Lond. A 219 (1953) 186–203.

[4] S. Whitaker, Theory and Applications of Transport in Porous Media: The Method of Volume Averaging, Kluwer Academic Publishers, 1999.

[5] I. Toumi, A. Bergeron, D. Gallo, E. Royer, D. Caruge, Flica-4: a three-dimensional two-phase flow computer code with advanced numerical methods for nuclear applications, Nucl. Eng. Des. 200 (2000) 139–155.

[6] W.T. SHA, An overview on rod-bundle thermal–hydraulic analysis, Nucl. Eng. Des. 62 (1980) 1–24.

[7] H. Darcy, Les fontaines publiques de Dijon, Dalmont, Paris, 1856.

[8] G. Taylor, The dispersion of matter in turbulent flow through a pipe, Proc. Roy. Soc. Lond. A 223 (1954) 446–468.

[9] R.G. Carbonell, S. Whitaker, Dispersion in pulsed system, part 2: theoritical developments for passive dispersion in porous media, Chem. Eng. Sci. 38 (11) (1983) 1795–1802.

[10] C. Mei, J.-L. Auriault, C. Ng, Some applications of the homogenization theory, Adv. Appl. Mech. 32 (1996) 278–348.

[11] J.-L. Auriault, P. Royer, Double conductivity media: a comparison between phenomenological and homogenization approaches, Int. J. Heat Mass Transfer 36 (10) (1993) 2613–2621.

[12] H. Brenner, Dispersion resulting from flow through spatially periodic porous media, Trans. Roy. Soc. 297 (1430) (1980) 81–133.

[13] V.S. Travkin, Discussion: "Alternative models of turbulence in a porous medium and related matters (D.A. Nield, 2001, ASME J. Fluids Eng. 123, pp. 928–931)", J. Fluids Eng. 123 (2001) 931–934.
[14] A. Nakayama, F. Kuwahara, A macroscopic turbulence model for flow in a porous medium, J. Fluids Eng. 121 (1996) 427–433.
[15] B. Wood, F. Cherblanc, M. Quintard, S. Whitaker, Volume averaging for determining the effective dispersion tensor: closure using periodic unit cells and comparison with ensemble averaging, Water Resour. Res. 39 (2005) 1154–1173.
[16] S. Whitaker, Diffusion and dispersion in porous media, AIChE 13 (3) (1967) 420–427.
[17] R.G. Carbonell, S. Whitaker, Heat and mass transfer in porous media, in: J. Bear, M.Y. Corapcioglu (Eds.), Fundamentals of Transport Phenomena in Porous Media, Martinus Nijhoff Publishers, 1984.
[18] O.A. Plumb, S. Whitaker, Dispersion in heterogeneous porous media. 1. Local volume averaging and large scale averaging, Water Resour. Res. 24 (7) (1988) 913–926.
[19] R. Aris, On the dispersion of a solute in a fluid flowing through a tube, Proc. Roy. Soc. Lond. A 235 (1956) 67–77.
[20] K.Y. Chien, Predictions of channel and boundary layer flows with a low reynolds number turbulence model, AIAA J. 20 (1) (1982) 33–38.
[21] C. Nagano, Y. Kim, A two equation model for heat transport in wall turbulent shear flows, J. Heat Transfer 110 (1988) 583–589.
[22] B.E. Launder, Heat and mass transport, in: P. Bradshaw (Ed.), Topics in Applied Physics: Turbulence, vol. 12, Springer-Verlag, 1976, pp. 232–289.
[23] H. Reichardt, Vollständige darstellung der turbulenten geschwindigkeitsverteilung in glaten leitungen, Z. Angew. Math. Mech. 31 (1951) 208–219.
[24] D. Laurence, V. Boyer, A shape function approach for high- and low-Reynolds near-wall turbulence model, Int. J. Numer. Methods Fluids 40 (2002) 241–251.
[25] P. Chassaing, Turbulence en mécanique de fluides: analyse du phénomène en vue de sa modélisation à l'usage de l'ingénieur, CEPADUES EDITIONS, 2000.
[26] H. Schlichting, K. Gersten, Boundary Layer Theory, 8th revised and enlarged edition., Springer, 2000.
[27] M. Quintard, S. Whitaker, Transport in ordered and disordered porous media: volume-averaged equations, closure problems and comparison with experiment, Chem. Eng. Sci. 48 (1993) 2537–2564.
[28] W.G. Gray, A. Leijnse, R.L. Kolar, C.A. Blain, Mathematical Tools for Changing Spatial Scales in the Analysis of Physical Systems, CRC Press, Boca Raton, FL, 1993.
[29] C.M. Marle, On macroscopic equations governing multiphase flow with diffusion and chemical reactions in porous media, Int. J. Eng. Sci. 20 (5) (1982) 643–662.
[30] M. Quintard, S. Whitaker, Transport in ordered and disordered porous media 2: generalized volume averaging, Transport Porous Media 14 (1994) 179–206.
[31] C. Moyne, S. Didierjean, H.P. Amaral Souto, O.T. Da Silveira, Thermal dispersion in porous media: one-equation model, Int. J. Heat Mass Transfer 43 (2000) 3853–3867.